Crystal Structures of the Ribonuclease MC1 Mutants N71T and N71S in Complex with 5′-GMP: Structural Basis for Alterations in Substrate Specificity†

Tomoyuki Numata,*,‡,§ Akio Suzuki,§,|| Yoshimitsu Kakuta,‡,⊥ Kazumi Kimura,‡ Min Yao,|| Isao Tanaka,|| Yuichiro Yoshida,@ Tadashi Ueda,@ and Makoto Kimura‡

Laboratory of Biochemistry, Department of Bioscience and Biotechnology, Faculty of Agriculture, Graduate School, Kyushu University, Fukuoka 812-8581, Japan, Division of Biological Sciences, Graduate School of Science, Hokkaido University, Sapporo 060-0810, Japan, RIKEN Harima Institute/SPring-8, 1-1-1 Koto, Mikazuki-cho, Sayo-gun, Hyogo 679-5148, Japan, and Graduate School of Pharmaceutical Sciences, Kyushu University, Fukuoka 812-8582, Japan

Received January 20, 2003; Revised Manuscript Received March 6, 2003

ABSTRACT: Ribonuclease MC1 (RNase MC1), isolated from bitter gourd seeds, is a uridine specific RNase belonging to the RNase T2 family. Mutations of Asn71 in RNase MC1 to the amino acids Thr (N71T) and Ser (N71S) in guanosine preferential RNases altered the substrate specificity from uridine specific to guanosine specific, as shown by the transphosphorylation of diribonucleoside monophosphates [Numata, T., et al. (2001) *Biochemistry 40*, 524−530]. To elucidate the structural basis for the alteration of substrate specificity, crystal structures of the RNase MC1 mutants N71T and N71S, free or complexed with 5′-GMP, were determined at resolutions higher than 2 Å. In the N71T−5′-GMP and N71S−5′-GMP complexes, the guanine moiety was, as in the case of the uracil moiety bound to wild-type RNase MC1, firmly stabilized in the B2 site by an extensive network of hydrogen bonds and hydrophobic interactions. Structure comparisons showed that mutations of Asn71 to Thr or Ser cause an enlargement of the B2 site, which then make it feasible to insert a guanine base into the B2 site of mutants N71T and N71S. This binding further allows for hydrogen bonding interaction of the side chain hydroxyl groups of Thr71 or Ser71 with the N7 atom of the guanine base. The mode of guanine binding of mutants N71T and N71S was found to be essentially identical to that of a guanosine preferential RNase NW from *Nicotiana glutinosa*. In particular, hydrogen bonds between the N7 atom of the guanine base and the hydroxyl groups of the amino acids at position 71 (RNase MC1 numbering) were completely conserved in three guanosine preferential enzymes, thereby indicating that the hydrogen bond may play an essential role in guanine binding in guanosine preferential RNases in the RNase T2 family. Consequently, it can be concluded that amino acids at position 71 (RNase MC1 numbering) serve as one of the determinants for substrate specificity (or preference) in the RNase T2 fimily by changing the size and shape of the B2 site.

One of the challenging subjects in ribonucleases (RNases) is to generate a novel base specific enzyme via protein engineering. To date, efforts have been directed mainly toward a guanine specific RNase T1[1] from *Aspergillus oryzae* (*1*) as a prototype. However, attempts to alter the substrate specificity of this enzyme have been unsuccessful (*2*−*6*), though the mode of binding of the substrate has been investigated in great detail (*7*−*10*).

Ribonuclease MC1 (RNase MC1, EC 3.1.27.1), isolated from the seeds of bitter gourd (*Momordica charantia*), is a small globular protein composed of 190 amino acids with a relative molecular mass of 21 188 Da (*11*) and belongs to the RNase T2 family typified by fungal RNases, such as RNase T2 from *A. oryzae* (*12*) and RNase Rh from *Rhizopus niveus* (*13*). RNase MC1 specifically cleaves a phosphodiester bond of single-stranded RNA at the 5′-side of uridine; dinucleoside monophosphates, NpU (where N is either A, C, G, or U), are minimum substrates of RNase MC1 (*14*). This absolute uridine specificity of RNase MC1 distinguishes it from other RNases in the RNase T2 family, which cleave almost all of the 16 dinucleoside monophosphates at a comparable rate, though all do show a unique base preference (*15*). In addition, the specificity of RNase MC1 set by uracil at the 3′-terminal side of dinucleoside monophosphates is distinct from those of other RNases, including those in RNase

† This study was supported in part by research fellowships of the Japan Society for the Promotion of Science for Young Scientists to T.N. (9157).

* To whom correspondence should be addressed: Laboratory of Biochemistry, Department of Bioscience and Biotechnology, Faculty of Agriculture, Graduate School, Kyushu University, Hakozaki 6-10-1, Higashi-ku, Fukuoka 812-8581, Japan. Telephone and fax: +81-92-642-2853. E-mail: rinsei@agr.kyushu-u.ac.jp.

‡ Graduate School, Kyushu University.

§ These authors contributed equally to the work.

|| Hokkaido University.

⊥ RIKEN Harima Institute/SPring-8.

@ Graduate School of Pharmaceutical Sciences, Kyushu University.

[1] Abbreviations: 5′-GMP, 5′-monophosphate guanylic acid; CpU, cytidylyl-3′,5′-uridine; CpG, cytidylyl-3′,5′-guanosine; BMGY, buffered glycerol complex medium; BMMY, buffered methanol complex medium; MD, minimal dextrose medium; MM, minimal methanol medium; PEG, polyethylene glycol; rms, root-mean-square; RNase MC1, ribonuclease MC1 from bitter gourd seeds; RNase NW, RNase NW from *N. glutinosa* leaves; RNase T1, RNase T1 from *A. oryzae*; SDS−PAGE, sodium dodecyl sulfate−polyacrylamide gel electrophoresis; YNB, yeast nitrogen base.

10.1021/bi034103g CCC: $25.00
Published on Web 04/18/2003

A and RNase T1 families. In general, RNases have two distinct base binding sites, the primary site (B1 site) and the subsite (B2 site), for bases located at the 5′- and 3′-sides of the scissile bond, respectively. Base specificity usually is related to the nature of the interaction of the B1 site with the base located at the 5′-side of the scissile bond (*16*). Thus, a strong interaction between the B2 site and the uracil at the 3′-side of the scissile phosphodiester bond is also a characteristic feature found in RNase MC1.

The crystal structure analysis of the RNase MC1 in complex with uridylic acids identified amino acids involved in uracil binding at the B2 site (*17*). The side chains of Gln9 and Asn71 interact with the uracil base by forming hydrogen bonds with O4 and N3 of uracil, respectively. The main chain amide nitrogen atom of Val72 also forms a hydrogen bond with O4 of uracil. Additionally, the side chains of Leu73 and Phe80 form a hydrophobic pocket, which is responsible for uracil binding by hydrophobic interactions. Subsequent mutagenesis studies demonstrated the role of these amino acids in substrate binding, and in particular, Asn71 was found to be highly responsible for uracil binding (*18*, *19*). Since amino acids at position 71 (RNase MC1 numbering) are variant in RNase T2 family enzymes, we assumed that Asn71 in RNase MC1 is strongly related to its uridine specificity at the B2 site. In our foregoing study, Asn71 in RNase MC1 was therefore replaced with amino acids Thr and Ser in guanosine preferential RNase NW from *Nicotiana glutinosa* (*20*) and RNase LX from tomato cultured cells (*21*), respectively, and the resulting mutants, N71T and N71S, respectively, were characterized in terms of substrate specificity. As was expected, both mutants N71T and N71S acquired guanine specificity, as shown from the transphosphorylation of diribonucleoside monophosphates (*18*). To our knowledge, this was the first success in producing a novel RNase with altered nucleotide specificity using protein engineering.

In this work, we attempted to elucidate the structural basis for alterations of the base specificity of mutants N71T and N71S. For this, we determined the crystal structures of the mutants, free or in complex with 5′-GMP, and compared the structural details with those of the wild-type RNase MC1, free or with a ligand with uridylic acids. In addition, the crystal structures of the mutants were compared with that of RNase NW in complex with 5′-GMP (*22*), and a role for the amino acid at position 71 (RNase MC1 numbering) in base recognition was discussed.

MATERIALS AND METHODS

Materials. Restriction enzymes were purchased from MBI Fermentas. The oligonucleotide primers and thermo sequenase fluorescent labeled primer cycle sequencing kits containing 7-deaza-dGTP were obtained from Amersham Pharmacia Biotech. The plasmid pGEM-T vector and expression plasmid pPIC9K were obtained from Promega and Invitrogen, respectively. The methylotrophic yeast *Pichia pastoris* GS115 was used as a host cell for producing the mutant N71T. 5′-Monophosphate guanylic acid (5′-GMP) and PEG8000 were purchased from Sigma Chemicals and Fluka Chemicals, respectively. Crystal Screen kits were obtained from Hampton Research. All other common chemicals and reagents were purchased at the highest available grade of purity.

Protein Preparation. The mutant N71S was produced in *Escherichia coli* and purified to homogeneity, as described previously (*18*). The mutant N71T was produced using the yeast *P. pastoris* expression system. The cDNA fragments encoding the mutant N71T were amplified by PCR using the full-length cDNA template and two oligonucleotide primers, 5′-AGATGAATTCGATTCCTTTTGGTTCGTCCA-3′ and 5′-ATATTTATTTTGCGGCCGCATCAAAAGATG-3′ as sense and antisense primers, respectively. The resulting product was subcloned into the pGEM-T vector. After confirmation of the cDNA sequence, using the dideoxy terminator sequencing method (*23*), plasmid DNA was digested with *Eco*RI and *Not*I. The cDNA fragments thus obtained were ligated in-frame into the *Eco*RI and *Not*I cloning sites in the expression vector pPIC9K to fuse the target protein with the α-factor signal sequence of yeast to secrete it into the growth medium. The resulting plasmid was digested with *Bgl*II to transform *P. pastoris* strain GS115, using the lithium chloride method. The transformants were selected from the histidine deficient medium (MD medium) (1.34% YNB, 4×10^{-5}% biotin, and 2% dextrose) as well as by the phenotype that slowly metabolized methanol (Mut^S, methanol utilization slow). Mut^S selection was carried out using MD medium and MM medium (1.34% YNB, 4×10^{-5}% biotin, and 0.5% methanol); the screened transformants grew normally in MD medium, but there was little or no growth in MM medium. A further selection was based on RNA hydrolysis activity on RNase indicator plates containing MM medium supplemented with 50 mg of toluidine blue O and 2 g of yeast RNA per liter (*24*). After the transformant was grown in 100 mL of BMGY medium [1% yeast extract, 2% peptone, 100 mM potassium phosphate (pH 6.0), 1.34% YNB, 4×10^{-5}% biotin, and 1% glycerol] for 2 days, the culture was inoculated into 1 L of BMMY medium [1% yeast extract, 2% peptone, 100 mM potassium phosphate (pH 6.0), 1.34% YNB, 4×10^{-5}% biotin, and 0.5−1.0% methanol] at an OD_{600} of 1.0. The culture was grown at 30 °C for 5 days, and we added 100% methanol to a final concentration of 0.5−1.0% every 24 h to maintain induction. After the growth medium had been centrifuged at 6000 rpm for 20 min, the supernatant was salted out using ammonium sulfate. The precipitated form was dialyzed against 10 mM sodium phosphate buffer (pH 6.5) and then purified to apparent homogeneity by a series of chromatography steps as in the case of the recombinant RNase MC1 expressed in *E. coli* (*18*).

After purification, both mutants N71T and N71S were dialyzed against distilled water and then concentrated to ∼12−16 mg/mL with a Centriprep apparatus (Amicon). The purity of the recombinant proteins was confirmed by SDS−PAGE using a 15% polyacrylamide gel (*25*). The N-terminal amino acid sequence was determined using a PSQ-1 gas-phase protein sequencer (Shimadzu). Protein concentrations were determined using bicinchoninic acid methods (*26*), with BSA as a standard protein.

Crystallization and Data Collection. The RNase MC1 mutants, free or complexed with 5′-GMP, were crystallized at 20 °C using the hanging drop vapor diffusion method by mixing 2 μL of protein solution (12−16 mg/mL in water) and 2 μL of reservoir solution in the absence or presence of 10 mM 5′-GMP. The crystals of the unliganded N71T grew within 1 week to a size of 0.8 mm × 0.5 mm × 0.15 mm

Table 1: Crystallographic Statistics of the RNase MC1 Mutants, Free or Complexed with 5′-GMP

	N71T	N71T−5′-GMP	N71S−5′-GMP
space group	$P2_12_12$	$P2_12_12_1$	$P2_12_12_1$
unit cell dimensions (Å)	$a = 58.8$ $b = 135.9$ $c = 52.4$	$a = 38.4$ $b = 65.8$ $c = 75.9$	$a = 38.5$ $b = 66.2$ $c = 75.5$
wavelength (Å)	1.0	1.0	0.9
resolution (Å)	35.81−1.65	50−1.5	32.81−1.6
R_{merge}[a,b]	0.053 (0.240)	0.087 (0.201)	0.157 (0.233)
no. of observed reflections	434769	156924	134016
no. of unique reflections	50905	31008	25113
multiplicity[a]	8.5 (5.7)	5.1 (4.5)	5.3 (2.3)
$I/\sigma(I)$[a]	9.0 (22.3)	15.7 (3.0)	8.6 (1.4)
completeness (%)[a]	99.2 (97.6)	98.5 (92.9)	95.6 (72.9)

[a] Values in parentheses represent data from the highest-resolution shell (1.74−1.65 Å for N71T, 1.55−1.5 Å for the N71T−5′-GMP complex, and 1.66−1.6 Å for the N71S−5′-GMP complex). [b] $R_{merge} = \Sigma(I - \langle I \rangle)/\Sigma(I)$, where I is the intensity measuremant for a given reflection and $\langle I \rangle$ is the average intensity for multiple measurements of this reflection.

against a reservoir containing 10 mM manganese chloride tetrahydrate and 30% (w/v) PEG1540. Crystallization conditions of the mutant enzymes in the presence of 5′-GMP were initially screened by the sparse-matrix sampling method using Crystal Screen kits from Hampton Research. Needles of the N71T−5′-GMP complex were obtained under condition 9, whereas small crystals of the N71S−5′-GMP complex were formed under condition 28 of the Crystal Screen kit. The conditions were then optimized to obtain large single crystals. Finally, the crystals of N71T in complex with 5′-GMP were grown to a size of 0.5 mm × 0.3 mm × 0.2 mm within 2 weeks against a reservoir containing 0.2 M ammonium acetate, 0.1 M trisodium citrate (pH 5.6), and 27.5% (w/v) PEG8000. The crystals of N71S with a ligand to 5′-GMP were grown within 4 days to 0.3 mm × 0.3 mm × 0.2 mm against a reservoir containing 0.2 M sodium acetate, 0.1 M sodium cacodylate (pH 6.5), and 24% (w/v) PEG8000.

The data set for a single crystal of unliganded N71T was collected at room temperature using the synchrotron radiation source at the BL40B2 station of SPring-8. As for the N71T−5′-GMP and N71S−5′-GMP complexes, single crystals were flash-frozen in a stream of liquid nitrogen, after which X-ray diffraction data were collected at 100 K at the BL44B2 and BL44XU stations of SPring-8, respectively. Data for unliganded N71T were processed using MOSFLM (*27*) and programs of the CCP4 suite (*28*), and those of the N71T−5′-GMP and N71S−5′-GMP binary complexes were integrated and scaled with HKL2000 (*29*) and d*TREC (*30*), respectively. Results of data reduction are summarized in Table 1.

Structure Determination. The structure of unliganded N71T was determined by molecular replacement using the program AMoRe (*31*), and those of the N71T−5′-GMP and N71S−5′-GMP complexes were determined by molecular replacement using the software package CNS (*32*). The structure of RNase MC1 [PDB entry 1BK7 (*33*)], from which the solvent had been removed, served as a search model. After protein atoms were refined by simulated annealing, the position and conformation of the 5′-GMP were clearly determined in the difference density maps of both N71T−5′-GMP and N71S−5′-GMP complexes. Structure refinements of unliganded N71T, the N71T−5′-GMP complex, and the N71S−5′-GMP complex were carried out using CNS and data from 10 to 1.65, 19.04 to 1.6, and 32.81 to 1.6 Å resolution, respectively. Iterative cycles of refinement and manual rebuilding in O (*34*) were carried out until the free *R*-factor converged. The topology restraints of 5′-GMP were from HIC-Up of Uppsala (*35*) and applied during refinement. The stereochemistry of the models was verified using PROCHECK (*36*).

Protein Data Bank Entries. The atomic coordinates of the N71T−5′-GMP and N71S−5′-GMP complexes have been deposited in the Protein Data Bank as entries 1J1F and 1J1G, respectively.

RESULTS

Preparation of Mutants. The mutant N71S was produced in *E. coli* and purified to apparent homogeneity, as described previously (*18*). Since yields of recombinant RNase MC1 and its mutants produced in *E. coli* cells were less than 0.5 mg per liter of culture broth (*18*, *19*, *37*), it seems likely that their productions may be uncongenial to the *E. coli* expression system. To circumvent the problem of small yields of the RNase MC1 mutants and also to undertake structural studies on the RNase MC1 mutants, we attempted to construct a functional expression system for the mutant N71T, using the methylotrophic yeast *P. pastoris*, as described in Materials and Methods. As a result, *P. pastoris* secreted the mutant N71T into the medium, and the protein was purified to apparent homogeneity in a series of chromatography studies. The yield of the mutant N71T was ∼7 mg/L of culture broth, demonstrating that the *P. pastoris* expression system is useful for preparation of a large amount of the RNase MC1 mutant. The direct N-terminal sequencing of the mutant N71T gave an amino acid sequence of Glu-Ala-Glu-Ala-Tyr-Val-Glu-Phe-Asp-Ser, indicating that the seven extra amino acids derived from the α-factor signal sequence were attached to the N-terminus (Phe) of the enzyme. Ribonucleolytic activity of the mutant N71T expressed in *P. pastoris* was confirmed using dinucleoside monophosphate CpG as a substrate (data not shown), the most favorable substrate for the mutant N71T.

Quality of the Structures. X-ray diffraction data were collected using an oscillation method at SPring-8 as described in Materials and Methods. As summarized in Table 1, the crystal of unliganded N71T has a form different from that of native crystals ($P2_12_12_1$); it belongs to space group $P2_12_12$ containing two molecules of unliganded N71T per asymmetric unit (V_M value of 2.45 Å^3/Da) with the following unit cell dimensions: $a = 58.79$ Å, $b = 135.90$ Å, and $c = 52.39$ Å. The current best diffraction data from the crystals of N71T−5′-GMP and N71S−5′-GMP complexes were collected up to 1.5 and 1.6 Å, respectively. Both crystals belong to orthorhombic space group $P2_12_12_1$ with the following unit cell parameters: $a = 38.4$ Å, $b = 65.8$ Å, and $c = 75.9$ Å in the crystals of the N71T−5′-GMP complex and $a = 38.5$ Å, $b = 66.2$ Å, and $c = 75.5$ Å in the crystals of the N71S−5′-GMP complex (Table 1). These unit cell dimensions were consistent with one monomer in the asymmetric unit; V_M values of the crystals of mutants N71T and N71S in complex with 5′-GMP were 2.18 and 2.27 Å^3/Da, respectively.

Table 2: Final Refinement Statistics

	N71T	N71T−5′-GMP	N71S−5′-GMP
resolution range (Å)	10.0−1.65	19.04−1.6	32.81−1.6
completeness (%)	99.1	98.3	94.2
no. of reflections	50618	25575	24732
total no. of non-hydrogen atoms			
protein	2984	1504	1491
5′-GMP		24	48
Mn	4		
solvent molecules	231	153	199
refinement			
R (%)[a]	18.1	22.1	21.7
R_{free} (%)[b]	19.5	24.4	24.2
rms deviations from ideal values			
bond lengths (Å)	0.004	0.005	0.005
bond angles (deg)	1.26	1.30	1.30
average overall isotropic B factors (Å^2)			
main chain atoms	21.8	15.6	12.9
side chain atoms	24.7	17.9	15.1
5′-GMP		22.4	31.8
Mn	42.2		
solvent molecules	35.1	29.3	28.3

[a] R (%) $= \sum|F_o - F_c|/\sum F_o$, where F_o and F_c are the observed and calculated structure factor amplitudes, respectively. [b] R_{free} was calculated for R, using only an unrefined subset of reflection data (5%).

FIGURE 1: Omit $F_o - F_c$ map in the vicinity of the B2 sites of N71T. The electron density map of N71T at 1.6 Å resolution was produced by omitting 5′-GMP from the model during map calculation, contoured at the 3.0σ level. The electron density map was calculated with CNS (*32*). This figure was generated with PyMOL (http://pymol.sourceforge.net/).

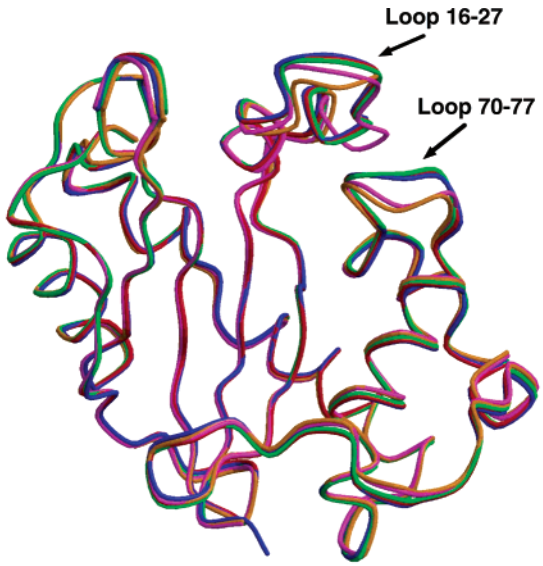

FIGURE 2: Superimposition of the overall structures of wild-type RNase MC1 and RNase MC1 mutants in the liganded and unliganded states. The RNase MC1−2′-UMP complex (green), the N71T−5′-GMP complex (blue), the N71S−5′-GMP complex (red), unliganded N71T molecule A (orange), and unliganded N71T molecule B (magenta) are shown. For simplicity, unliganded wild-type RNase MC1 is not shown, because no structural changes were observed upon binding of uridylic acids to wild-type RNase MC1. The loops of residues 16−27 and 70−77 exhibiting significant conformational changes between the N71T−5′-GMP complex and unliganded N71T are labeled. The rms deviations for α-carbon atoms among these proteins are summarized in Table 3. This figure was produced with MOLSCRIPT (*40*) and Raster 3D (*41*).

The crystal structure of unliganded N71T was determined at 1.65 Å resolution by molecular replacement using RNase MC1 (1BK7) as a search model. The structure of N71T was refined to R and R_{free} values of 0.181 and 0.195, respectively, for the 10−1.65 Å resolution range (Table 2). The refined structure of N71T included 231 water molecules and four Mn^{2+} ions. The rms deviations from ideal bond lengths and angles of N71T were 0.004 Å and 1.26°, respectively.

Both crystal structures of N71T−5′-GMP and N71S−5′-GMP complexes were determined at 1.6 Å resolution. 5′-GMP was clearly present in the B2 sites within both mutants, as seen in omit $F_o - F_c$ maps (Figure 1). After localization of 153 water molecules, the structure of N71T in complex with 5′-GMP was refined to an R of 0.221 and an R_{free} of 0.244 at 1.6 Å resolution (Table 2). The model of N71S with a ligand to 5′-GMP has an R of 0.217 and an R_{free} of 0.242 for the data in the 32.81−1.6 Å resolution range, including 199 water molecules. The rms deviations from ideal values are 0.005 Å for bond lengths and 1.3° for bond angles in both N71T−5′-GMP and N71S−5′-GMP complexes (Table 2).

It should be noted that two 5′-GMP molecules were bound to the protein in the N71S−5′-GMP complex: one to the B2 site of N71S, which is a specific interaction between the B2 site and the guanine base, and the other bound to the opposite side of the active site by an extensive network of hydrogen bonds with the side chains of Ser63, Thr67, and Asn110, and in addition by a symmetry-related hydrogen

Table 3: Root-Mean-Square Deviations among Each Protein[a]

	RNase MC1−2′-UMP	unliganded N71T	
		molecule A	molecule B
N71T−5′-GMP	0.306	0.667	0.634
N71S−5′-GMP	0.218	0.656	0.615
unliganded N71T			
molecule A	0.591	−	0.452
molecule B	0.574	0.452	−

[a] The values are calculated by the Lsq_explicit command in O and expressed in angstroms.

bond with the side chain of Lys140. It was therefore suggested that the latter 5′-GMP molecule plays an important role in crystal packing. This assumption is consistent with the finding that no crystal of N71S grew in the absence of 5′-GMP.

Comparison of Protein Structures. The crystal structure of unliganded N71T is essentially identical to that of the wild-type RNase MC1 (1BK7), except for the loop structure around the B2 site (residues 70−77) and its proximal loop between residues 16 and 27, as shown in Figure 2. Thus, the mutation caused a slight conformational change in the loop structures. The crystal structures of RNase MC1 in complex with uridylic acids showed that the side chain of Asn71 interacts with the main chain carbonyl oxygen of Asn76 as well as with the uracil base. It was thus assumed that the conformational change observed in the mutant N71T may be due to a loss of hydrogen bonding interactions between the side chain of Thr71 and the main chain of Asn76 in the mutant N71T.

The overall structures of N71T−5′-GMP and N71S−5′-GMP complexes could be superimposed with an rms deviation of 0.201 Å (Figure 2). We then examined the effects of 5′-GMP binding on the conformation of the guanine binding loop by comparing the structures of the N71T−5′-GMP complex and N71T. As shown in Figure 2, positional differences in backbone atoms were observed around the base binding loop (residues 70−77) and adjacent N-terminal loop region (residues 16−27). The differences in Cα positions are up to 3.36 Å (residue 75 C-α), and the main chain rms deviations are 0.634−0.667 Å (Table 3). Therefore, the loop structure containing Thr71 undergoes a conformational change on guanine binding and the accompanying movement of the proximal loop structure at positions 16−27.

Structures of N71T−5′-GMP and N71S−5′-GMP complexes were then compared with that of the wild-type RNase MC1−2′-UMP complex (Figure 2 and Table 3). Structures of both N71T−5′-GMP and N71S−5′-GMP complexes were very similar to that of the RNase MC1−2′-UMP complex: main chain rms deviations of 0.306 (N71T) and 0.218 Å (N71S). These findings indicate that the conformation of the loop around residues 70−77 in N71T changed to the wild-type form with the binding of 5′-GMP. Taken together, the mutation of Asn71 resulted in deformation of the loop structure, and the 5′-GMP binding recovered the conformation identical to that of RNase MC1 as well as RNase MC1 in complex with uridylic acids.

Binding Mode of 5′-GMP. In both N71T−5′-GMP and N71S−5′-GMP complexes, 5′-GMP is bound to the active site, and the glycosyl torsion angle of 5′-GMP adopts a syn conformation (Figure 3). In both complexes, the mutant proteins interact with the guanine moiety by an extensive

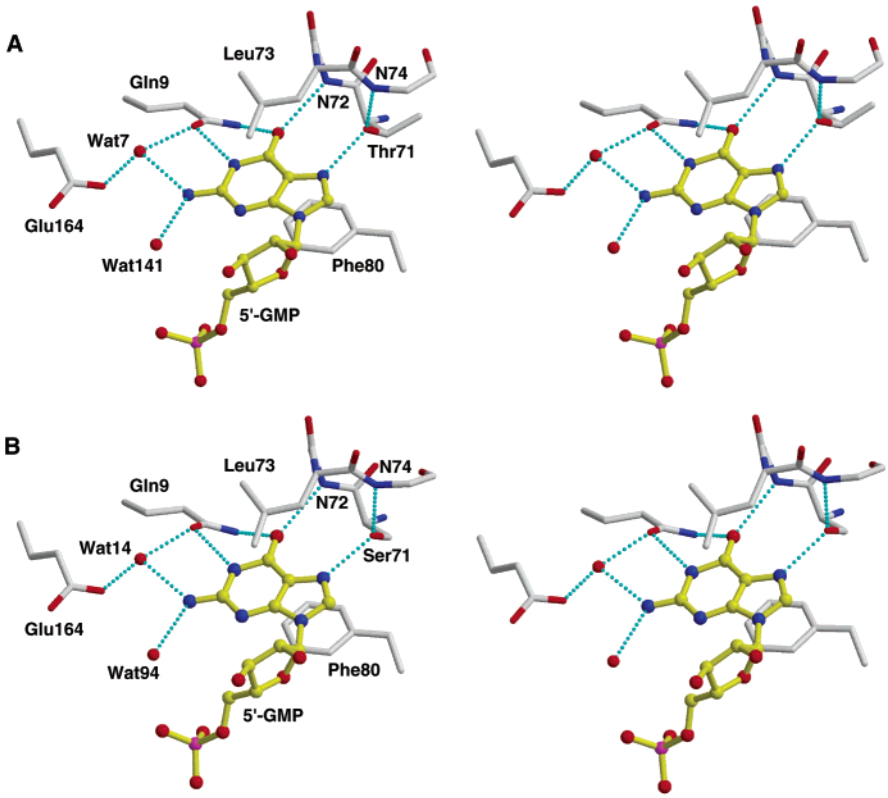

FIGURE 3: Stereoviews of the binding mode of 5′-GMP at the B2 sites in the RNase MC1 mutants N71T (A) and N71S (B). Amino acids are shown as sticks (white); 5′-GMP is shown as a ball and stick (yellow), and water molecules are shown as balls. Val72 and Arg74, the only main chain atoms, are shown. Oxygen atoms are in red, nitrogen atoms in blue, and phosphorus atoms in magenta. Dotted lines represent hydrogen bonds. Hydrogen bond distances between the RNase MC1 mutants and 5′-GMP are listed in Table 4.

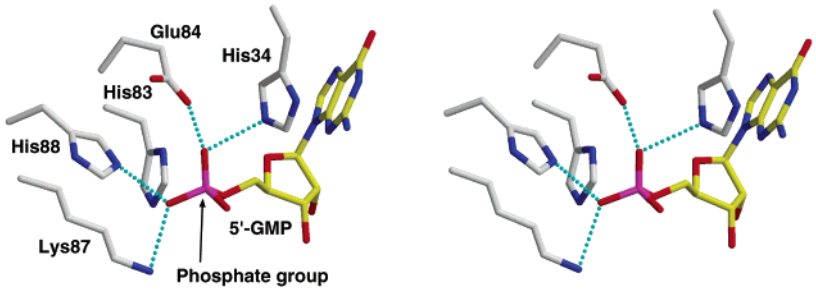

FIGURE 4: Stereoview of the intermolecular interaction between catalytic residues in N71T and the phosphate group of 5′-GMP. 5′-GMP is drawn in yellow, and amino acid side chains are drawn in white. Interactions are shown as dotted lines. The phosphate moiety of 5′-GMP tightly interacts with catalytic residues of the RNase MC1 mutant. The geometry of bound 5′-GMP in the N71S−5′-GMP complex is almost identical to that of the N71T−5′-GMP complex.

hydrogen bond network. The side chain amide oxygen atom of Gln9 serves as a hydrogen acceptor from N1H of the guanine base. The O6 atom of the guanine base forms hydrogen bonds with the side chain amide nitrogen of Gln9 and the backbone nitrogen atom of Val72. The side chain hydroxyl group of Thr71 (or Ser71) donates a hydrogen bond to the N7 atom of the guanine moiety. The side chain hydroxyl oxygen atom of Thr71 (or Ser71) also accepts a hydrogen bond from the main chain amide nitrogen atom of Arg74, thereby indicating that the orientation of the side chain of the amino acid at position 71 is stabilized so that it specifically interacts with the guanine base. Furthermore, the N2 atom of the guanine base donates hydrogen bonds to two water molecules, one of which in turn forms hydrogen bonds to the side chain amide oxygen atom of Gln9 and the side chain carboxyl group of Glu164. In addition, the guanine moiety lies between the two hydrophobic amino acid residues, Leu73 and Phe80.

The phosphate moiety of 5′-GMP is located around the catalytic residues of RNase MC1 (Figure 4). This finding, together with the observation that the guanine base is firmly fixed at the B2 site, suggests that the mode of interaction between the mutant enzymes and 5′-GMP may be appropriate for enzymatic reaction. Therefore, N71T and N71S are assumed to be capable of acquiring catalytic efficiency (k_{cat}/K_m) toward CpG at a rate comparable to that of wild-type RNase MC1 toward CpU (*18*). In contrast to the guanine moiety and the phosphate group, no apparent interactions were present between the mutant proteins and the ribose moiety of 5′-GMP. Hydrogen bond distances between the mutant enzymes and 5′-GMP are summarized in Table 4.

Comparison of Base Binding Sites. The amino acid residues involved in the interaction with bases in the B2 sites of three complexes, RNase MC1−2′-UMP, N71T−5′-GMP, and N71S−5′-GMP, are superimposed in Figure 5. The guanine moiety of 5′-GMP binds at B2 sites of N71T and N71S in a position almost identical to that of the uracil base in the RNase MC1−2′-UMP complex, except that the *N*-glycosyl linkage shifts its position by 1.8−2.3 Å. This movement in the position of the *N*-glycosyl linkage in the mutants is essential for binding of the guanine moiety to the B2 sites because of the bulkiness of the guanine base relative to uracil.

The binding mode of uracil observed in the RNase MC1−2′-UMP complex is conserved in the mutant enzymes in complex with 5′-GMP. Namely, four of five hydrogen bonds formed in the RNase MC1−2′-UMP complex are conserved in both mutant enzymes in complex with 5′-GMP: Gln9 Nε2···guanine O6, Val72 NH···guanine O6, water···Gln9 Oε1, and water···Glu164 Oε1. In addition, the side chains of Leu73 and Phe80 interact with the nucleotide base by hydrophobic interaction. However, N71T and N71S have additional interactions with the guanine base, as compared with that of RNase MC1 with the uracil base. First, three hydrogen bonds, Oε1 of Gln9 with N1H of guanine and two water-mediated hydrogen bonds with N2H1 and N2H2 of guanine, are additionally formed in both mutant enzymes. Second, the mutation of Asn71 to Thr or Ser led to expansion of the base binding site, thereby making it possible to insert a larger guanine base into the B2 site of these mutant enzymes. This further resulted in formation of a novel hydrogen bond between the side chain hydroxyl group of Thr or Ser at position 71 and the N7 atom of the guanine moiety in both complexes.

Table 4: Hydrogen Bond Interactions of 5′-GMP with the RNase MC1 Mutants and Solvents

5′-GMP atom	residue atom	distance (Å)	
		N71T	N71S
guanine base			
N1	Gln9 Oε1	2.92	3.02
N2	Wat7	2.94	
	Wat14		2.97
N2	Wat141	3.00	
	Wat94		3.03
O6	Val72 N	2.88	2.84
O6	Gln9 Nε2	2.99	3.05
N7	Thr71 Oγ1	2.60	
	Ser71 Oγ		2.67
phosphate			
O1P	His34 Nε2	2.88	2.85
O1P	Glu84 Oε2	2.48	2.50
O3P	Lys87 Nζ	2.75	2.66
O3P	His88 Nε2	3.02	3.00

As described, the mutant N71T was generated on the basis of the finding that the guanine preferential RNase NW from *N. glutinosa* leaves has Thr in place of Asn71 in RNase MC1. Recently, the crystal structure of RNase NW in complex with 5′-GMP was determined at 1.5 Å resolution (*22*). So, we compared the guanine binding site in RNase NW with that in N71T. In the crystal structure, RNase NW formed a ligand with 5′-GMP, the guanine moiety of 5′-GMP is bound in the B2 site of RNase NW, and the glycosyl bond of 5′-GMP is in the syn conformation as in the cases of N71T and N71S. Hydrophobic interactions as well as an extensive hydrogen bond network observed in the RNase NW−5′-GMP complex are closely similar to those of the guanosine specific mutants N71T and N71S (Figure 6), except that the side chain of

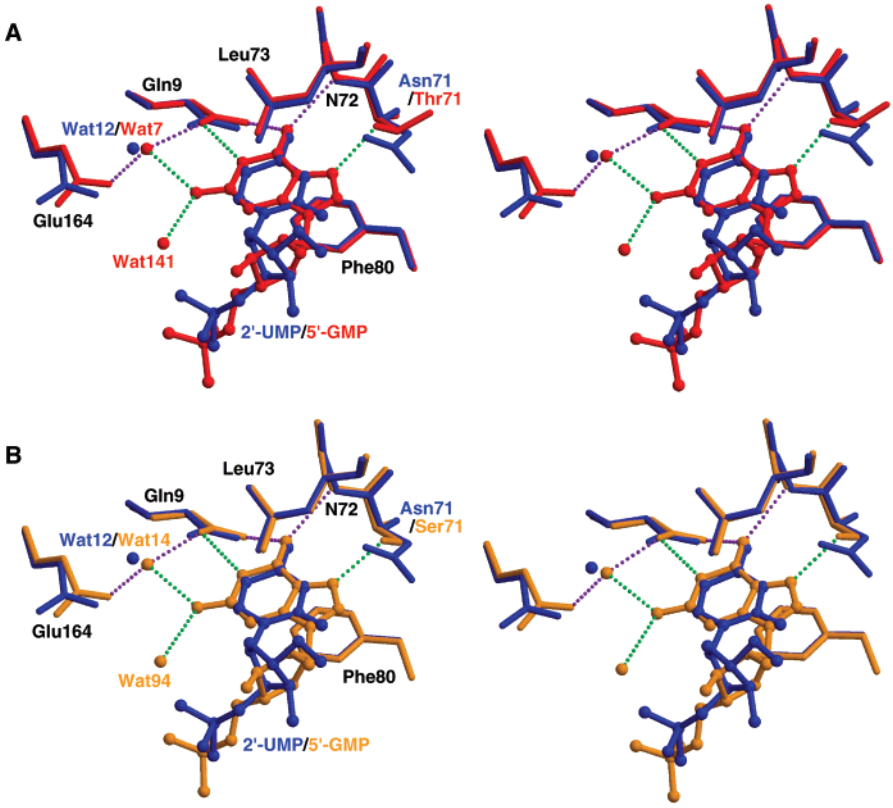

FIGURE 5: Structural comparison of the mode of base binding in wild-type RNase MC1 and the mutants. (A) Stereoview of superimposed structures of the RNase MC1−2′-UMP (blue) and N71T−5′-GMP (red) complexes and (B) stereoview of superposition of RNase MC1−2′-UMP (blue) and N71S−5′-GMP (orange) complexes. Proteins are shown in a stick model; 5′-GMP is shown as a ball and stick, and water molecules are shown as balls. Dotted lines in both figures represent hydrogen bonds formed between the RNase MC1 mutants (N71T and N71S) and 5′-GMP. The hydrogen bonds shown in purple are conserved among the wild-type and mutant RNase MC1, whereas those shown in green are specific interactions observed in the mutant enzymes in complex with 5′-GMP. The amino acid mutations of Asn71 to Thr and Ser cause enlargements of the B2 sites in the mutant proteins, resulting in binding of the guanine moiety to the base recognition site.

Tyr17 in RNase NW lies in an equivalent position of Leu73 of RNase MC1, participating in the hydrophobic interaction with the guanine base. In particular, the N7 atom of the guanine base hydrogen bonds to the hydroxyl group of Thr78 of RNase NW, corresponding to the amino acid at position 71 of RNase MC1. This hydrogen bond is also formed between the mutants of RNase MC1 and the N7 atom of guanine (Figure 6), indicating that the side chains of Thr71 and Ser71 in the RNase MC1 mutants interact with the guanine base in a manner identical to that of Thr78 in RNase NW. In addition, the orientation and position of 5′-GMP in the active site of the three complexes are essentially identical. This is consistent with the finding that catalytic efficiencies for the cleavage of CpG by N71T and N71S were comparable to that of the wild-type RNase MC1 toward CpU (*18*). In conclusion, structural analyses presented here strongly demonstrate that the amino acids at position 71 (in RNase MC1 numbering) serve as one of the determinants of substrate specificity in the RNase T2 family enzymes by adjusting the size of the B2 site.

DISCUSSION

Structural Basis for Base Specificities. The mutations of Asn71 in the B2 site in the uridine specific RNase MC1 to Thr and Ser in the guanine specific RNases resulted in generation of a novel RNase with guanine specificity (*18*). These structural analyses of the mutants revealed that the mutations of Asn by Thr and Ser enlarge the space of the B2 site, and this allows the guanine base to insert into the B2 site in the mutants. The accessible surface areas of the mutant enzymes around the B2 site are 128 (N71T) and 125 Å^2 (N71S), which are increased by 1.36- and 1.33-fold, respectively, in comparison to that of wild-type RNase MC1 (94 Å^2). The volume of the B2 sites in the mutant enzymes is likely to be an adequate size for specific binding of the guanine base, and they can stabilize the guanine moiety at the B2 site by forming an extensive network of hydrogen bonds. Consequently, the mutations of Asn71 to Thr and Ser resulted in alteration of the substrate specificity from uridine specific to guanosine specific due to these specific interactions with the guanine base.

Conversely, the spaces of the B2 sites in the mutant enzymes are too large for uracil to tightly bind the B2 site. Although it is premature to discuss it precisely without knowing the crystal structure of the mutant enzymes in complex with uridylic acids, N3H of the uracil moiety may have no direct interaction with the hydroxyl group of the amino acid at position 71 in the mutant enzymes, because they may be too distant to form hydrogen bonds. Therefore, the mutant enzymes N71T and N71S may loosely recognize the uracil base, the result being decreases in enzymatic activity toward CpU of 16- and 5.9-fold, respectively, as compared with that of wild-type RNase MC1 (*18*).

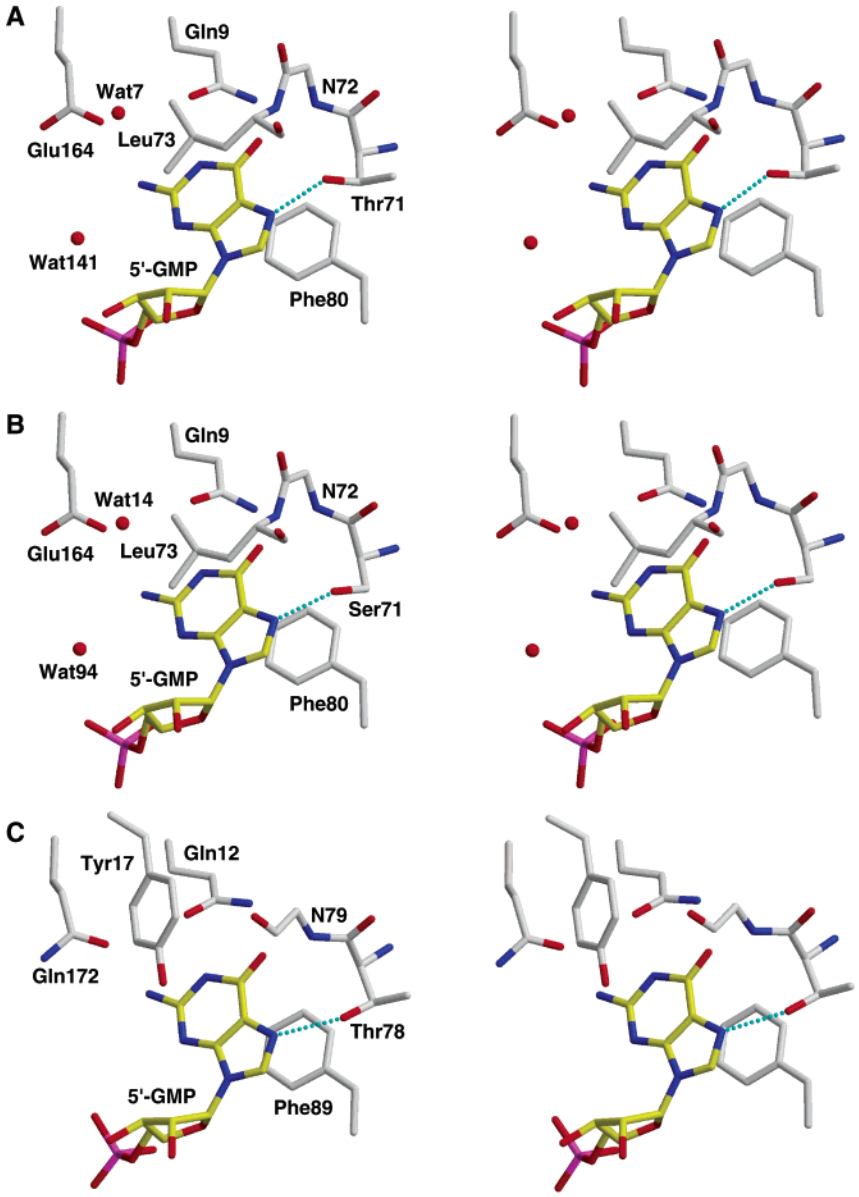

FIGURE 6: Comparison of guanosine binding in the RNase MC1 mutants with that of RNase NW. Shown are the mode of 5′-GMP binding of RNase MC1 mutants N71T (A) and N71S (B) and RNase NW (C) in stereo representation. The side chains of Val72 in RNase MC1 mutants and Leu79 in RNase NW (corresponding to Val72 in RNase MC1) are omitted. Atoms are shown in the standard colors. Dotted lines represent hydrogen bonds formed between N7 atoms of the guanine base and the hydroxyl group of the side chains of amino acid residues at position 71 (RNase MC1 numbering).

The mutants N71T and N71S showed no enzymatic activity toward dinucleoside monophosphates CpA and CpC (*18*). The binding mode of 5′-GMP in these mutant enzymes provides an explanation for the rejection of both adenine and cytosine bases from their B2 sites. Nϵ2 of Gln9 and the backbone nitrogen atom of Val72 are unable to form hydrogen bonds with N6H1 or N6H2 of the adenine base, and in addition, water-mediated hydrogen bonds to N2H1 and N2H2 of guanine base are missing in adenine−protein interactions because of a lack of an amino group at position 2 of the adenine base. It is thus impossible to interact with the adenine base at the B2 site, though sizes of the B2 sites in both mutant proteins are probably suitable for adenine binding. With respect to cytosine, the B2 sites of the mutant proteins are too large to interact with cytosine. Moreover, the hydrogen bond network observed in the complexes of N71T and N71S with 5′-GMP may not be stabilized in the interaction with cytosine, as the cytosine base has an amino group at position 6, with no interactions with the backbone nitrogen atom of Val72. It is thus likely that the little activity of N71T and N71S toward CpA and CpC may be due to a destabilization of a hydrogen bond network between B2 sites and bases.

Possible Explanations for the Alteration of Substrate Specificity of RNase MC1. As described above, despite many attempts to change the substrate specificity of RNase T1, RNase T1 mutants with an altered nucleotide specificity have not been generated (*2*−*6*). For example, the mutation of Glu46 in RNase T1 to Gln resulted in a narrowing of the guanine recognition site, thus preventing the formation of two hydrogen bonds with a guanine base (*4*). As a result, RNase T1 mutant E46Q interacts with 2′-GMP not in the specific recognition site (B1 site) but in the B2 site. Nevertheless, the base specificity of the mutant E46Q was not altered. Hahn and co-workers generated RNase T1 variant 9/5 by random mutagenesis on the guanine recognition site

(*5*) and determined its crystal structure in complex with 2′-GMP (*38*), revealing that the guanine moiety was slightly shifted in plane out of the guanine binding pocket by ~1 Å, though it was fixed to the B1 site of RNase T1. As a result of the altered geometry of 2′-GMP binding in RNase T1 variant 9/5, the phosphate group of 2′-GMP cannot be properly positioned to the active site and located ~4.2 Å away from its position in the wild-type RNase T1−2′-GMP complex. In this manner, mutations of the guanine recognition site of RNase T1 could not alter the base specificity because of the inappropriate binding mode of the base, which further forces the phosphate group out of the active site.

In our previous study, the mutation of Asn71 in RNase MC1 to the corresponding amino acids in guanosine preferential RNases produced a novel RNase with altered substrate specificity (*18*). It was noteworthy that only a single amino acid substitution resulted in a change in the nucleotide specificity from uridine specific to guanosine specific. The reasons for a successful alteration of nucleotide specificity of RNase MC1 are assumed to be as follows. First, RNase MC1 has no absolute base specificity compared with RNase T1, though it preferentially cleaves at the 5′-side of uridine. In contrast, RNase T1 has a pronounced specificity for guanine. Kinetic studies on RNase T1 revealed that the specificity constant (k_{cat}/K_m) for GpN is ~10^6-fold greater than that for ApN and at least 10^8-fold greater than that for CpN and UpN (*39*). In contrast, the specificity constant of RNase MC1 for CpU is only ~350-fold greater than that of CpG (*18*). It is therefore likely that a successful alteration of the base specificity of RNase MC1 may be due in part to its specificity ratio being lower than that of RNase T1.

Second, a hydrogen bond network formed between RNase MC1 and the base moiety is mainly mediated by side chains rather than by main chain atoms. In contrast, RNase T1 tightly interacts with the guanine base at the B1 site by an extensive network of hydrogen bonds mainly formed by main chain atoms. It is therefore expected that RNases, like RNase MC1, which recognize a base by forming hydrogen bonds mainly using its side chains, would be good candidates for protein engineering of a prototype to generate novel RNases with a distinct base specificity.

ACKNOWLEDGMENT

We thank Drs. Atsushi Nakagawa and Eiki Yamashita of Osaka University (Osaka, Japan) and Dr. Taiji Matsu of the RIKEN Harima Institute for their help with data collection using synchrotron radiation at beamlines BL44XU and BL44B2 of SPring-8. We are grateful to M. Ohara (Fukuoka, Japan) for helpful comments on the manuscript.

REFERENCES

1. Sato, K., and Egami, F. (1957) *J. Biochem. 44*, 753−767.
2. Nishikawa, S., Morioka, H., Kimura, T., Ueda, Y., Tanaka, T., Uesugi, S., Hakoshima, T., Tomita, K., Ohtsuka, E., and Ikehara, M. (1988) *Eur. J. Biochem. 173*, 389−394.
3. Grunert, H. P., Landt, O., Zirpel-Giesebrecht, M., Backmann, J., Heinemann, U., and Saenger, W., and Hahn, U. (1993) *Protein Eng. 6*, 739−744.
4. Granzin, J., Puras-Lutzke, R., Landt, O., Grunert, H. P., Heinemann, U., Saenger, W., and Hahn, U. (1992) *J. Mol. Biol. 225*, 533−542.
5. Hubner, B., Haensler, M., and Hahn, U. (1999) *Biochemistry 38*, 1371−1376.
6. Kumar, K., and Walz, F. G., Jr. (2001) *Biochemistry 40*, 3748−3757.
7. Heinemann, U., and Saenger, W. (1982) *Nature 299*, 27−31.
8. Arni, R., Heinemann, U., Tokuoka, R., and Saenger, W. (1988) *J. Biol. Chem. 263*, 15358−15368.
9. Heydenreich, A., Koellner, G., Choe, H. W., Cordes, F., Kisker, C., Schindelin, H., Adamiak, R., Hahn, U., and Saenger, W. (1993) *Eur. J. Biochem. 218*, 1005−1012.
10. Koepke, J., Maslowska, M., Heinemann, U., and Saenger, W. (1989) *J. Mol. Biol. 206*, 475−488.
11. Ide, H., Kimura, M., Arai, M., and Funatsu, G. (1991) *FEBS Lett. 284*, 161−164.
12. Uchida, T. (1966) *J. Biochem. 60*, 115−132.
13. Tomoyeda, M., Eto, Y., and Yoshino, T. (1969) *Arch. Biochem. Biophys. 131*, 191−202.
14. Irie, M., Watanabe, H., Ohgi, K., Minami, Y., Yamada, H., and Funatsu, G. (1993) *Biosci., Biotechnol., Biochem. 57*, 497−498.
15. Irie, M. (1999) *Pharmacol. Ther. 81*, 77−89.
16. Steyaert, J. (1997) *Eur. J. Biochem. 247*, 1−11.
17. Suzuki, A., Yao, M., Tanaka, I., Numata, T., Kikukawa, S., Yamasaki, N., and Kimura, M. (2000) *Biochem. Biophys. Res. Commun. 275*, 572−576.
18. Numata, T., Suzuki, A., Yao, M., Tanaka, I., and Kimura, M. (2001) *Biochemistry 40*, 524−530.
19. Numata, T., and Kimura, M. (2001) *J. Biochem. 130*, 621−626.
20. Kariu, T., Sano, K., Shimokawa, H., Itoh, R., Yamasaki, N., and Kimura, M. (1998) *Biosci., Biotechnol., Biochem. 62*, 1144−1151.
21. Löffler, A., Glund, K., and Irie, M. (1993) *Eur. J. Biochem. 214*, 627−633.
22. Kawano, S., Kakuta, Y., and Kimura, M. (2002) *Biochemistry 41*, 15195−15202.
23. Sanger, F., Nickelsen, S., and Coulson, A. R. (1977) *Proc. Natl. Acad. Sci. U.S.A. 74*, 5463−5467.
24. Quaas, R., Laudt, O., Grunert, H.-P., Beineke, M., and Hahn, U. (1989) *Nucleic Acids Res. 17*, 3318.
25. Laemmli, U. K. (1970) *Nature 227*, 680−685.
26. Smith, P. K., Krohn, R. I., Hermanson, G. T., Mallia, A. K., Garther, F. K., Provenzano, M. D., Fujimoto, E. K., Goeke, N. M., Olson, B. J., and Klenk, D. C. (1985) *Anal. Biochem. 150*, 76−85.
27. Leslie, A. G. W. (1992) *Joint CCP4/ESF-EACMB Newsletter on Protein Crystallography 26*.
28. Collaborative Computational Project Number 4 (1994) *Acta Crystallogr. D50*, 760−763.
29. Otwinowski, Z., and Minor, W. (1997) *Methods Enzymol. 276*, 307−326.
30. Pflugrath, J. W. (1999) *Acta Crystallogr. D55*, 1718−1725.
31. Navaza, J. (1994) *Acta Crystallogr. A50*, 157−163.
32. Brunger, A. T., Adams, P. D., Clore, G. M., DeLano, W. L., Gros, P., Grosse-Kunstleve, R. W., Jiang, J. S., Kuszewski, J., Nilges, M., Pannu, N. S., Read, R. J., Rice, L. M., Simonson, T., and Warren, G. L. (1998) *Acta Crystallogr. D54*, 905−921.
33. Nakagawa, A., Tanaka, I., Sakai, R., Nakashima, T., Funatsu, G., and Kimura, M. (1999) *Biochim. Biophys. Acta 1433*, 253−260.
34. Jones, T. A., Zou, J. Y., Cowan, S. W., and Kjeldgaard, M. (1991) *Acta Crystallogr. A47*, 110−119.
35. Gerard, J. K., and Jones, T. A. (1998) *Acta Crystallogr. D54*, 1119−1131 (CCP4 Proceedings).
36. Laskowski, R. A., MacArthur, M. W., Moss, D. S., and Thornton, J. M. (1993) *J. Appl. Crystallogr. 26*, 283−291.
37. Numata, T., Kashiba, T., Hino, M., Funatsu, G., Ishiguro, M., Yamasaki, N., and Kimura, M. (2000) *Biosci., Biotechnol., Biochem. 64*, 603−605.
38. Höschler, K., Hoier, H., Hubner, B., Saenger, W., Orth, P., and Hahn, U. (1999) *J. Mol. Biol. 294*, 1231−1238.
39. Walz, F. G., Osterman, H. L., and Libertin, C. (1979) *Arch. Biochem. Biophys. 195*, 95−102.
40. Kraulis, P. J. (1991) *J. Appl. Crystallogr. 24*, 946−950.
41. Merrit, E. A., and Murphy, M. E. P. (1994) *Acta Crystallogr. D50*, 869−873.

BI034103G